Local field effects in half-metals: A *GW* study of zincblende CrAs, MnAs, and MnC

L. Damewood* and C. Y. Fong

Department of Physics, University of California Davis, One Shields Avenue, Davis, California 95616-8677, USA

(Received 19 May 2010; revised manuscript received 16 February 2011; published 22 March 2011)

We used the *GW* approximation to examine the improvements of the semiconducting gap in three predicted half-metals with the zincblende structure, CrAs, MnAs and MnC, compared to density-functional theory with the generalized gradient approximation. Recognizing the differences in the local field effect between transition metals and insulators, respectively, we modeled one spin channel in a half-metal as metallic having a *d* character and the oppositely oriented spin channel as insulating. To demonstrate the necessity of treating these three compounds as having a *d* character, we also applied the *GW* approximation to CrAs using the nearly free electron model in the conducting channel. We found that CrAs shows the least improvement, while Mn-based half-metals exhibit comparable improvements. Physical explanations for these results are presented.

DOI: 10.1103/PhysRevB.83.113102 PACS number(s): 73.20.At, 68.35.−p, 75.50.Cc

Half-metals, first predicted by de Groot *et al.*,[1] are a promising class of materials for spintronic applications due to their inherently large (and integer unit Bohr magneton) magnetic moments ($\geqslant 1.0\mu_B$) and complete spin polarization at the Fermi energy E_F. One spin channel of a half-metal has a partially filled valence band, like a metal, while the oppositely oriented spin channel has a completely filled valence band, like an insulator or a semiconductor, resulting in 100% spin polarization at E_F. Types of half-metallic compounds theoretically predicted so far include some Heusler alloys,[2] such as Co_2FeSi, NiMnSb, and PtMnSb;[1] some Si containing half–Heusler alloys with Curie temperatures over 600K,[3] such as NiCrSi and PdCrSi; some transition-metal oxides, including rutile structured CrO_2;[4,5] some perovskites,[6] such as $LaMnO_3$ and $SeMnO_3$; and a few more simply structured zincblende (ZB) compounds, including CrAs[7] and superlattices. NiMnSb[9] and CrO_2[10] have been experimentally determined to be half-metals at very low temperatures.

ZB CrAs was first predicted to be a half-metal and then grown in thin-film form by Akinaga *et al.*[7] It has many desirable properties that make it a good candidate for half-metallic based spintronic devices: it has a simple stoichiometry and is, thus, easier to control; it has a large magnetic moment of $3\mu_B$ and an experimentally estimated Curie temperature of over 400 K, well above room temperature; and it can be epitaxially grown as a thin film on a GaAs substrate.[7] Unfortunately, ZB half-metals are meta-stable and do not exist in bulk form, since the ZB structure is not the ground state.

Despite their meta-stability, ZB half-metals have inspired many theoretical studies. Pask *et al.*[11] studied CrAs, along with MnAs, MnC, and other ZB materials, using pseudopotential and LAPW calculations with a generalized gradient approximation (GGA) exchange-correlation functional.[12] GGA and local density approximation functionals are, however, known to underestimate the semiconducting gap. Additionally, devices containing half-metals will have a biasing or gate voltage during operation, so knowledge of the gap will determine an upper limit for the devices' operating voltages. To determine an accurate band gap in half-metals, we turn to the so-called *GW* method,[13] which is known to recover from the underestimated band gap of semiconductors and insulators.[14] In general, the improvement to the gap due to the *GW* method depends on the separation and the electronegativity difference between ions.[15]

The *GW* method is a many-body approach for electronic structure calculations that describes weakly interacting quasiparticles obeying the following equation:

$$h(x)\phi_i(x) + \int dx' \Sigma(x,x')\phi_i(x') = \epsilon_i \phi_i(x), \qquad (1)$$

where $h(x)$ is the single-particle Hamiltonian; $\phi_i(x)$ and ϵ_i are the quasiparticle wave functions and energies, respectively; and $\Sigma(x,x')$ is the nonlocal, energy-dependent self-energy, which includes local-field effects. Due to inhomogeneities in electron density on a scale smaller than the conventional unit cell, localized electric fields can polarize charges in insulators and semiconductors. These local fields are described by the off-diagonal ($\mathbf{G} - \mathbf{G}' \neq 0$) elements of the momentum $\mathbf{q}$, dependent dielectric matrix

$$\epsilon(\mathbf{q}+\mathbf{G},\mathbf{q}+\mathbf{G}'), \qquad (2)$$

where $\mathbf{G}$ and $\mathbf{G}'$ are reciprocal lattice vectors. In metals, where the electron density does not vary substantially over short distances, the local-field effect is small and the off-diagonal matrix elements of the dielectric matrix may be ignored.[16]

The *GW* approach, in part by accurately accounting for local-field effects and dynamical effects—such as the polarization of the electron gas due to a moving electron—has been extremely successful in improving the energy gap in semiconductors and insulators determined by local density approximation or GGA and agreeing with measurements of quasiparticle energies and lifetimes by direct or inverse photoemission experiments.[14] Within the *GW* approximation (GWA), complicated many-body vertex corrections are neglected and the self-energy is represented by the simple convolution $\Sigma = GW$, where G is the quasiparticle propagator and $W = \epsilon^{-1} V_{\text{Coulomb}}$ is the screened Coulomb potential.

While half-metals have properties of metals and insulators, approximations within the *GW* method have only been applied to systems that are either fully insulating or metallic. The conventional *GW* approach should be modified to treat the simultaneous existence of both types of electronic properties in half-metals. In this paper, we investigate how the physical characteristics of the local fields in ZB half-metals and the

improvement of the semiconducting gap depends on the choice of transition metal and nonmetallic elements.

Due to the separate metallic and insulating spin channels, we treat the local-field effect in each spin channel differently. In particular, the half-metallic irreducible polarization P(Half-metallic), is split between contributions from each spin channel:

$$P(\text{Half-metallic}) = \sum_{\sigma} P_{\sigma} = P_1(\text{Metallic}) + P_2(\text{Insulating}). \quad (3)$$

The separation of the spin channels allows for the exclusion of local fields in the metallic channel while maintaining the treatment of local-field effects in the other spin channel. Instead, if the material is an insulator, both spin channels are insulating and the fully insulating polarization would be

$$P(\text{Fully Insulating}) = P_1(\text{Insulating}) + P_2(\text{Insulating}). \quad (4)$$

The issue still remains whether the metallic channel in a ZB half-metal should be treated in the nearly free electron model (simple metal), where only a single, $\mathbf{G} = 0$ vector is required,[17] or as a transition metal, where localized d electrons require the inclusion of many $\mathbf{G}$ vectors in the form of diagonal matrix elements.[18]

By examining the charge density contributions near E_F in the metallic channel and near the top of the valence band in the insulating channel, we were able to justify the exclusion of the local fields in the metallic channel as well as determine if many or few $\mathbf{G}$ vectors are required to form the diagonal elements of the dielectric matrix. We used ZB CrAs as the prototypical example of the three ZB halfmetals. In Fig. 1, the densities of states of the spin channels in CrAs are given with E_F set to 0. In Fig. 2(a), we show the charge density contribution in ZB CrAs to the metallic channel near E_F and in Fig. 2(b), we show the charge density contribution in the insulating channel at the top

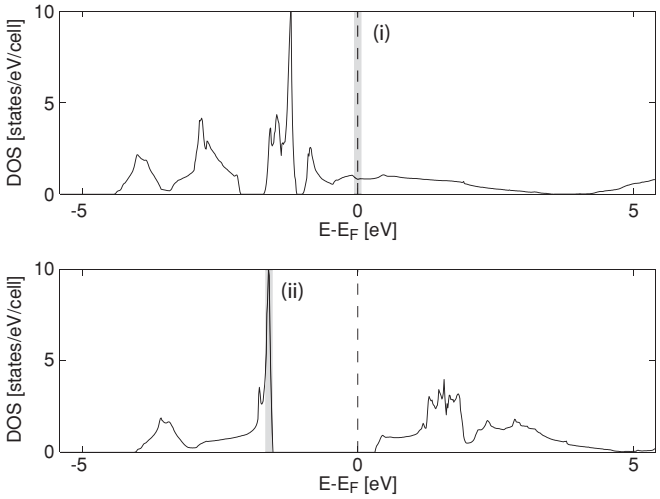

FIG. 1. Density of states of CrAs in (a) the majority spin channel and (b) the minority spin channel. (i) and (ii) denote where the partial charge density in Fig. 2 is taken from. (i) points out the 27.2-meV range around E_F in the metallic channel and (ii) points out the small 27.2-meV range at the top of the insulating channel valence band.

of the valence band E_{Top}, where the density of states is highest, as shown in Figure 1(b). The levels of the contours in both charge distributions in Fig. 2 are identical, so it is clearly seen that the distribution of charge in Fig. 2(a) is more homogeneous than the charge in Fig. 2(b). The uniformity of the charge density of the metallic channel compared to the insulating channel demonstrates that the electrons in the majority spin channel are not expected to contribute substantially to the local fields. These considerable differences in the charge density justify the separate treatments of the local-field effects in a ZB half-metal. Furthermore, the distribution of charge in Fig. 2(a) still exhibits some d character for these states near E_F. We are, therefore, not justified to treat the local-field effect due to the metallic channel using the nearly free electron model, but instead, we must treat this spin channel like a transition metal.

Our approach accounts for all diagonal contributions ($\mathbf{G} = \mathbf{G}'$) to the dielectric matrix for the metallic channel and the full dielectric matrix for the insulating channel. This differs from the usual *GW* method, in which the dielectric matrices for the two spin channels are treated as either both metallic or both insulating/semiconducting. For the purpose of comparison to the nearly free electron metal, we shall also calculate the GWA in CrAs, taking into account the extreme case of using only the $\mathbf{G} = \mathbf{G}' = 0$ contribution in the majority spin channel dielectric matrix, thereby treating the dielectric response as if the metallic channel has a uniform charge density.

The software package ABINIT[19,20] was utilized to carry out the one-shot, spin-polarized, GWA using the Godby-Needs plasmon-pole model.[21] We initialized the GWA with a set of eigenfunctions and eigenenergies using the ionic pseudopotentials determined from the projector augmented wave (PAW)[22] scheme, with the GGA as the exchange correlation functional. In all three ZB half-metals, we used a plane-wave cutoff of 1600 eV and a (20,20,20) Monkhorst-Pack[23] $\mathbf{k}$-point mesh such that the total energy was converged to within 1 meV. The lattice constant of the CrAs unit cell, 5.66 Å, was determined by finding the lattice constant that minimizes the total energy within the initial PAW calculation, while the lattice constants for MnAs (5.75 Å) and MnC (5.08 Å) were determined by finding lattice values that resulted in an integer magnetic moment. These results are in agreement with the previous studies by Pask *et al.*[11] and Qian *et al.*[24] In addition, the exchange part of the self-energy matrix, Σ_X, was constructed using wave functions with a cutoff of 430 eV of kinetic energy and the corresponding self-energy matrix used 2685 $\mathbf{G}$ vectors.

We used the conventional *GW* approach, with a 181 $\mathbf{G}$ vector dielectric matrix for each spin channel, to handle the insulating case. In the half-metallic case, we performed a similar calculation, but in accordance with our model, we excluded the off-diagonal matrix elements of the metallic dielectric matrix only, representing the weak local-field effect in that channel. To account for the extreme case of the nearly free electron model, an additional calculation was performed on CrAs that included only the $\mathbf{G} = \mathbf{G}' = 0$ term in the metallic-like channel.

Table I lists the values of the semiconducting gap using the PAW-determined psuedopotentials with the GGA and three treatments of the local-field effect: fully insulating, transition metal, and simple metal. The gap determined by

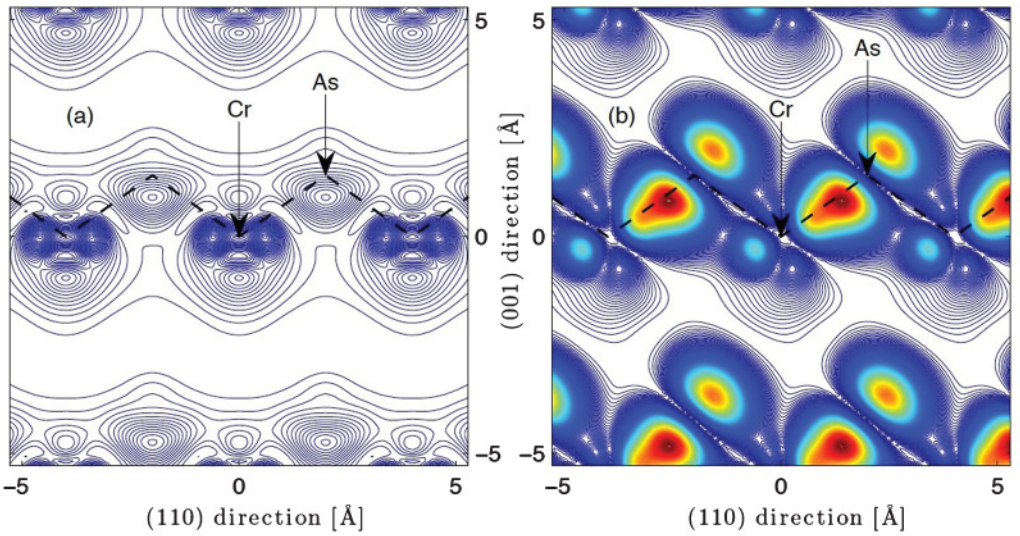

FIG. 2. (Color online) Charge density contributions in ZB CrAs (a) near E_F ($|E - E_F| \leqslant 13.6$ meV) in the majority spin channel and (b) at the top of the valence band, E_{Top} ($E_{Top} - 27.2\,\text{meV} \leqslant E \leqslant E_{Top}$), where the density of states is highest in the minority spin channel. Contour levels represent a difference of 0.02×10^{-5}electrons/cm^3 between lines. (a) The majority spin channel is relatively flat, with a maximum charge density of 0.54×10^{-5}electrons/cm^3, compared to (b) the minority spin channel, with a maximum charge density peak of 6.87×10^{-5}electrons/cm^3.

the simple-metal local field is presented for CrAs only. In general, the GGA exchange correlation functional is known to underestimate the gap by as much as 30%. In CrAs, the half-metallic local-field model widened the gap by 0.11 eV (6% increase), while the inclusion of the local field in the fully insulating local-field model was different by only 0.04 eV (2%), demonstrating that the local fields in the metallic channel are indeed negligible. The first two GWA calculations on CrAs are in remarkable contrast to the half-metallic local-field model with only the single $\mathbf{G} = \mathbf{G}' = 0$ vector, which widened the gap an additional 0.50 eV (23%). The widening of the gap in this case can be understood by the lack of participation of the metallic d electrons in the short-range screening of nuclear charges. When all but the long-range $\mathbf{G} = \mathbf{G}' = 0$ contributions are neglected, the localized d electrons in the metallic channel cannot easily screen the nuclear charge. The resulting Coulomb potential W causes the gap to increase by a significant amount. Since the metallic d electrons should screen the nuclear charge, the latter case is physically unreasonable and shorter-range diagonal matrix elements should be included.

TABLE I. Semiconducting gaps (in eV) for ZB CrAs using four methods: the GGA as the exchange correlation functional, the fully insulating local-field GWA, the half-transition-metal local-field GWA using only $\mathbf{G} = \mathbf{G}'$ reciprocal lattice vectors in the metallic spin channel, and the extreme case of the half-simple-metal local-field GWA using a single $\mathbf{G} = 0$ reciprocal lattice vector in the metallic spin channel. Semiconducting gaps for MnAs and MnC are also provided within the first three methods.

Half-metal	Method	Gap (eV)
CrAs	PAW + GGA	1.85
	Fully insulating local field	1.92
	Half-transition-metal local field	1.96
	Half-simple-metal local field	2.46
MnAs	PAW + GGA	1.70
	Fully insulating local field	2.07
	Half-transition-metal local field	2.21
MnC	PAW + GGA	1.55
	Fully insulating local field	2.07
	Half-transition-metal local field	2.22

The influence of the extra d electron in MnAs over CrAs explains both the greater increase in the GW gap over the GGA gap (0.52 eV in MnAs versus 0.11 eV in CrAs) and the 0.14 eV difference between the local-field models. In MnAs, the extra d electron produces a fourfold increase in the peak electronic charge density near E_F in the metallic channel compared to CrAs, illustrating the greater importance of the local fields. Likewise, MnC has a nearly identical electronic charge density peak in the metallic channel, suggesting a similar local-field effect. Additionally, MnC demonstrates how the electronegativity and the nearest-neighbor distance affect the GW-determined gap. The electronegativity of C (2.5) is twice as large as As[25] (1.25) and the lattice constant of MnC is much smaller than that of MnAs, resulting in a larger improvement over the GGA gap.

In summary, we have investigated the role of the local-field effect in ZB half-metals on the semiconducting gap using a modified GWA scheme based on the physical circumstances in half-metals. As electrons in the metallic channel are more delocalized than electrons in the insulating channel, the local-field effect represented by the off-diagonal matrix elements in the dielectric matrix in the metallic channel may be ignored. However, due to the d-state character of the metallic channel of ZB half-metals, the nonzero diagonal matrix elements ($\mathbf{G} = \mathbf{G}' \neq 0$) of the dielectric matrix yield a significant

contribution to the screening of nuclear charges. Among the three predicted half-metals, MnAs and MnC both show a larger improvement over CrAs due to the extra electron in the transition-metal element. The improvement in MnC is 0.15 eV larger than MnAs, owing to the differences in the electronegativity of the nonmetal elements and nearest-neighbor separation distance. The improved, widened semiconducting gap will enable experimentalists to apply proper bias or gate voltages when half-metallic compounds are used for devices.

This research was supported in part by the National Science Foundation under Grant No. ECCS-0725902. This work was also supported by the National Science Foundation through TeraGrid resources provided by the National Center for Supercomputing Applications (NCSA).

*Corresponding author: ldamewood@student.physics.ucdavis.edu

[1] R. A. de Groot, F. M. Mueller, P. G. van Engen, and K. H. J. Buschow, Phys. Rev. Lett. **50**, 2024 (1983).
[2] F. Heusler, Verh. Dtsch. Phys. Ges. **5**, 219 (1903).
[3] V. A. Dinh, K. Sato, and H. Katayama-Yoshida, J. Supercond. Novel Magn. **23**, 79 (2010).
[4] K. Schwarz, J. Phys. F **16**, L211 (1986).
[5] K. P. Kämper, W. Schmitt, G. Güntherodt, R. J. Gambino, and R. Ruf, Phys. Rev. Lett. **59**, 2788 (1987).
[6] J. Park, E. Vescovo, H. Kim, C. Kwon, and R. Ramesh, Nature **392**, 794 (1998).
[7] H. Akinaga, T. Manago, and M. Shirai, Jpn. J. Appl. Phys., Part 2 **39**, L1118 (2000).
[8] C. Y. Fong, M. C. Qian, J. E. Pask, L. H. Yang, and S. Dag, Appl. Phys. Lett. **84**, 239 (2004).
[9] C. Hordequin, D. Ristoiu, L. Ranno, and J. Pierre, Eur. Phys. J. B **16**, 287 (2000).
[10] Y. Ji, G. J. Strijkers, F. Y. Yang, C. L. Chien, J. M. Byers, A. Anguelouch, G. Xiao, and A. Gupta, Phys. Rev. Lett. **86**, 5585 (2001).
[11] J. E. Pask, L. H. Yang, C. Y. Fong, W. E. Pickett, and S. Dag, Phys. Rev. B **67**, 224420 (2003).
[12] J. P. Perdew, K. Burke, and M. Ernzerhof, Phys. Rev. Lett. **77**, 3865 (1996).
[13] L. Hedin, Phys. Rev. **139**, A796 (1965).
[14] M. S. Hybertsen and S. G. Louie, Phys. Rev. B **34**, 5390 (1986).
[15] T. Lu and J. Zheng, Chem. Phys. Lett. **501**, 47 (2010).
[16] J. E. Northrup, M. S. Hybertsen, and S. G. Louie, Phys. Rev. Lett. **59**, 819 (1987).
[17] J. E. Northrup, M. S. Hybertsen, and S. G. Louie, Phys. Rev. B **39**, 8198 (1989).
[18] F. Aryasetiawan, Phys. Rev. B **46**, 13051 (1992).
[19] X. Gonze, J. Beuken, R. Caracas, F. Detraux, M. Fuchs, G.-M. Rignanese, L. Sindic, M. Verstraete, G. Zerah, and F. Jollet, Comput. Mater. Sci. **25**, 478 (2002).
[20] X. Gonze, G. Rignanese, M. Vertraete, J. Beuken, Y. Pouillon, R. Caracas, F. Jollet, M. Torrent, G. Zerah, M. Mikami *et al.*, Z. Kristallogr. **220**, 558 (2005).
[21] R. W. Godby and R. J. Needs, Phys. Rev. Lett. **62**, 1169 (1989).
[22] P. E. Blöchl, Phys. Rev. B **50**, 17953 (1994).
[23] H. J. Monkhorst and J. D. Pack, Phys. Rev. B **13**, 5188 (1976).
[24] M. C. Qian, C. Y. Fong, and L. H. Yang, Phys. Rev. B **70**, 052404 (2004).
[25] J. C. Phillips, *Covalent Bonding in Crystals, Molecules, and Polymers* (University of Chicago Press, Chicago, 1969).